Inorg. Chem. **2002**, *41*, 180–191

$NaCeP_2Se_6$, $Cu_{0.4}Ce_{1.2}P_2Se_6$, $Ce_4(P_2Se_6)_3$, and the Incommensurately Modulated $AgCeP_2Se_6$: New Selenophosphates Featuring the Ethane-Like $[P_2Se_6]^{4-}$ Anion

Jennifer A. Aitken,[†] Michel Evain,[‡] Lykourgos Iordanidis,[†] and Mercouri G. Kanatzidis[†,*]

Department of Chemistry and Center for Fundamental Materials Research, Michigan State University, East Lansing, Michigan 48824, and I.M.N., UMR CNRS C6502, Institut des Matériaux Jean Rouxel, Laboratoire de Chimie des Solides, 2 rue de la Houssinière, BP 32229, 44322 Nantes Cedex 03, France

Received June 11, 2001

$NaCeP_2Se_6$, $Cu_{0.4}Ce_{1.2}P_2Se_6$, and $AgCeP_2Se_6$ were prepared from nearly stoichiometric proportions of the starting materials plus extra selenium at 750–850 °C. $Ce_{1.33}P_2Se_6$ (or $Ce_4(P_2Se_6)_3$) was obtained from the same reaction that produced $Cu_{0.4}Ce_{1.2}P_2Se_6$. The structure of all four compounds was determined by single-crystal X-ray diffraction. $NaCeP_2Se_6$, $Cu_{0.4}Ce_{1.2}P_2Se_6$, and $Ce_{1.33}P_2Se_6$ crystallize in the monoclinic space group, $P2_1/c$, with $a = 12.1422(2)$, $b = 7.6982(1)$, $c = 11.7399(2)$ Å, $\beta = 111.545(1)°$ and $Z = 4$ for $NaCeP_2Se_6$; $a = 12.040(1)$, $b = 7.6418(8)$, $c = 11.700(1)$ Å, $\beta = 111.269(2)°$ and $Z = 4$ for $Cu_{0.4}Ce_{1.2}P_2Se_6$; and $a = 6.8057(5)$, $b = 22.969(2)$, $c = 11.7226(8)$ Å, $\beta = 124.096(1)°$ and $Z = 6$ for $Ce_{1.33}P_2Se_6$. $NaCeP_2Se_6$ has a two-dimensional character and is isostructural to the $KLnP_2Q_6$ family of compounds, where Ln = La, Ce, and Pr for Q = Se and Ln = La for Q = S. The structure consists of $[CeP_2Se_6]_n^{n-}$ layers which are separated by Na^+ cations. Each layer contains $CeSe_9$ distorted, tricapped trigonal prisms and $[P_2Se_6]^{4-}$ ethane-like anions. $Cu_{0.4}Ce_{1.2}P_2Se_6$ possesses a similar structure; however, substitution of the alkali metal by copper and cerium atoms renders the structure three dimensional. $Ce_{1.33}P_2Se_6$ is the pure lanthanide member of this structure type. In this three-dimensional structure, there are three cerium metal sites which are partially occupied. The structure of $AgCeP_2Se_6$ was solved in the superspace group $P2_1/c(\alpha 0 \gamma)$ and represents an incommensurately modulated version of the $KLnP_2Q_6$ structure type, with $a = 9.971(5)$, $b = 7.482(3)$, $c = 11.757(4)$ Å, $\beta = 145.630(9)°$, $q = 0.3121(18)a^* + 0.4116(19)c^*$, and $Z = 2$. The structures of the compounds reported here and those of the $KLnP_2Q_6$ family are highly related to the monoclinic-II, $M^{II}PQ_3$ structure type (where M = Pb, Sn, Ca, and Sr for Q = S and M = Pb and Sn for Q = Se). Optical and vibrational spectroscopic characterization is also reported.

Introduction

Recently there has been a renewed interest in rare-earth chalcogenides.[1−5]Of particular interest to our research group are rare-earth chalcophosphates.[6] These materials comprise a relatively small class of compounds,[7−19] which have been prepared and investigated over the last 30 years. The family of $LnPS_4$ compounds (where Ln = Y, La, Ce, Pr, Nd, Sm, Gd, Tb, Er, Tm, and Yb)[7] stands out because of their interesting luminescent behavior. Also rather intriguing is the recent discovery that $KTbP_2Se_6$ exhibits a pressure-induced phase transition at ∼9.2 GPa.[15] It has been proposed that the high-pressure phase is due to charge transfer from the selenium to the phosphorus accompanied by the formation of a Se−Se bond.

* To whom correspondence should be addressed. E-mail: Kanatzid@cem.msu.edu.
† Michigan State University.
‡ Institut des Matériaux Jean Rouxel.

(1) Kumta, P. N.; Risbud, S. H. *J. Mater. Sci.* **1994**, *29*, 1135.
(2) Parkin, I. P.; Fitzmaurice, J. C. *Polyhedron* **1993**, *12*, 1569−1571.
(3) Chen, J. H.; Dorhout, P. K. *J. Solid State Chem.* **1995**, *117*, 318−322.
(4) Kanatzidis, M. G.; Sutorik, A. C. *Prog. Inorg. Chem.* **1995**, *43*, 151-265. (b) Aitken, J. A.; Cowen, J. A.; Kanatzidis, M. G. *Chem Mater.* **1998**, *10*, 3928−3935. (c) Choi, K. S.; Hanko, J. A.; Kanatzidis, M. G. *J. Solid State Chem.* **1999**, *147*, 309−319. (d) Patschke, R.; Brazis, P.; Kannewurf, C. R. *J. Mater. Chem.* **1999**, *9*, 2293−2296. (e) Iordanidis, L.; Kanatzidis, M. G. *Inorg. Chem.* **2001**, *40*, 1878−1887.
(5) Narducci, A. A.; Yang, Y. T.; Digman, M. A.; Sipes, A. B.; Ibers, J. A. *J. Alloy Compd.* **2000**, *303*, 432−439. (b) Huang, F. Q.; Brazis, P.; Kannewurf, C. R.; Ibers, J. A. *Inorg. Chem.* **2000**, *39*, 3176−3180. (c) Huang, F. Q.; Ibers, J. A. *J. Solid State Chem.* **2000**, *151*, 317−322.
(6) Kanatzidis, M. G. *Curr. Opin. in Solid State Mater. Sci.* **1997**, *2*, 139−149, and references therein.

10.1021/ic010618p CCC: $22.00 © 2002 American Chemical Society
Published on Web 12/28/2001

Initially, our goal was to synthesize selenium analogues of the $LnPS_4$ phases. In the process of our investigations into the Ce−P−Se system, we discovered $NaCeP_2Se_6$. This phase was formed when the starting materials reacted with the fused silica reaction tube and abstracted sodium ions. Later a more rational synthesis was devised. This surprise was well received since sodium containing selenophosphates are little known.[20] $NaCeP_2Se_6$ is isostructural to the $KLnP_2Q_6$ family of compounds, where Ln = La, Ce, and Pr for Q = Se[16] and Ln = La for Q = S.[17] The highly impressive tendency of this system to mine Na^+ ions in order to form a quaternary compound, rather than a ternary Ce−P−Se phase, emphatically underscored the considerable stability of this structure type and prompted us to prepare analogues with similarly charged and sized cations, e. g., Cu and Ag. Investigations with these coinage metals led to three other new phases, namely $Cu_{0.4}Ce_{1.2}P_2Se_6$, $AgCeP_2Se_6$, and $Ce_4(P_2Se_6)_3$, which will be referred to as $Ce_{1.33}P_2Se_6$ from here on. Albeit more intricate, $Cu_{0.4}Ce_{1.2}P_2Se_6$ and $Ce_{1.33}P_2Se_6$ are also related to the $KLnP_2Q_6$ structure type. Interestingly, $AgCeP_2Se_6$ presents a complicated crystallographic problem because it possesses an incommensurately modulated version of the $KLnP_2Q_6$ structure, which could only be solved accurately using the four-dimensional space group $P2_1/c$ $(\alpha 0 \gamma)$.

The structure of the compounds described here is highly related to the "monoclinic-II", $M^{II}PQ_3$ structure-type *($P2_1/c$)*,[21] where M = Pb,[22] Sn,[22] Ca,[23] and Sr[23] for Q = S and M = Pb[24] and Sn[25] for Q = Se. Several members of this structure type, such as $Sn_2P_2S_6$ and $Sn_2P_2Se_6$, show ferroelectric−paraelectric phase transitions and have recently attracted attention as promising materials for use in memory devices.[26] $(Pb_{0.45}Sn_{0.55})_2P_2Se_6$ is useful as a sensitive and tunable thermometer at low temperatures, as it is unaffected by large magnetic fields (up to 20 T).[27] Here we report the synthesis, structure, and optical and Raman spectroscopic properties of $NaCeP_2Se_6$, $Cu_{0.4}Ce_{1.2}P_2Se_6$, $Ce_{1.33}P_2Se_6$, and $AgCeP_2Se_6$.

Experimental Section

Reagents. The chemicals for this work were used as obtained unless noted otherwise: (i) sodium metal, analytical reagent, Mallinckrodt Inc., Paris, KY; (ii) copper metal powder, Fisher Scientific Company, Fair Lawn, NJ; (iii) silver metal 99.99%, Liberty Coins, Lansing, MI; (iv) cerium metal powder 99.9%, <250 micron, Alfa Aesar, Ward Hill, MA; (v) red phosphorus powder, 100 mesh, EM Science, Gibbstown, NJ; (vi) selenium powder 99.5+%, 100 mesh, Aldrich Chemical Co., Inc., Milwaukee, WI.

Synthesis. Ag Metal Powder. A silver coin (99.99%) was dissolved in 250 mL of hot 8.4 M nitric acid. This solution was neutralized to a pH of 6 with 150 mL of ammonium hydroxide. Next, 15 mL of formic acid was added over a time period of 30 min. The solution was allowed to stir at 50 °C for 2 h followed by filtering. The granular precipitate of silver was washed with ethanol and acetone and dried in vacuo.[28]

Na_2Se and P_2Se_5. Na_2Se and P_2Se_5 were prepared as described elsewere.[20,29]

Preparation of $NaCeP_2Se_6$. I. Initial Synthesis. In a nitrogen filled glovebox, 0.035 g (0.25 mmol) Ce, 0.342 g (0.75 mmol) P_2-

(7) $LnPS_4$ (where Ln = Y, La, Ce, Pr, Nd, Sm, Gd, Tb, Er, Tm, and Yb:) (a) Yampol′akaya, V. V.; Serebrennikov, V. V. *Russ. J. Inorg. Chem.* **1972**, *17*, 1771−1772. (b) Wibbelmann, C.; Brockner, W.; Eisenmann, B.; Schäfer, H. *Z. Naturforsch.* **1984**, *39a*, 190−194. (c) Palkina, K. K.; Maksimova, S. I.; Chibiskova, N. T.; Kuvshinova, T. B.; Volodina, A. N. *Inorg. Mater. Engl. Tr.* **1984**, *20*, 1557−1560. (d) Volodina, A. N.; Koubchinova, T. B.; Maximova, S. I.; Mouraviev, E. N.; Niazov, C. A.; Tchibiskova, N. I. *Zh. Neorg. Khim SSSR* **1987**, *32*, 2899−2901. (e) Le Rolland, B.; Molinié, P.; Colombet, P. *C. R. Acad. Sci. Paris Série II* **1990**, *310*, 1201−1206. (f) Le Rolland, B.; McMillan, P.; Molinié, P.; Colombet, P. *Eur. J. Solid State Inorg. Chem.* **1990**, *27*, 715−724. (g) Palkina, K. K.; Kuvshinova, T. B.; Maksimova, S. I.; Chibiskova, N. T.; Tirpolskaya, T. A. *Inorg. Mater. Engl. Tr.* **1989**, *25*, 1555-1556. (h) Huang, Z. L.; Victoria, C.; Pilippe M. *J. Rare Earth* **1999**, *17*, 6−11. (i) Huang, Z. L. *J. Rare Earth* **1998**, *16*, 167−171. (j) Huang, Z. L.; Cajipe, V. B.; LeRolland, B.; Colombet, P.; Schipper, W. J.; Blasse, G. *Eur. J. Solid State Inorg. Chem.* **1992**, *29*, 1133−1144.

(8) $Eu_2P_2S_6$: Brockner, W.; Becker, R. *Z. Naturforsch.* **1987**, *42a*, 511−512.

(9) $Eu_2P_2Se_6$ is mentioned briefly as a footnote in ref 16b.

(10) $TlEuPS_4$: Carrillo-Cabrera, W.; Peters, K.; von Schnering, H. G. *Z. Anorg. Allg. Chem.* **1995**, *621*, 557−561.

(11) $LiEuPSe_4$ and $KEuPSe_4$: Aitken, J. A.; Chondroudis, K.; Young, V. G. Jr.; Kanatzidis, M. G. *Inorg. Chem.* **2000**, *39*, 1525−1533.

(12) $K_4Eu(PSe_4)_2$: Chondroudis, K.; McCarthy, T. J.; Kanatzidis, M. G. *Inorg. Chem.* **1996**, *35*, 840−844.

(13) $Rb_9Ce(PSe_4)_4$: Chondroudis, K.; Kanatzidis, M. G. *Inorg. Chem. Commun.* **1998**, *1/2*, 55−57.

(14) $A_4RE_2(PSe_4)_2(P_2Se_6)$ (A = Rb, Cs; RE = Ce, Gd), $A_3RE(PSe_4)_2$ (A = Rb, Cs; RE = Ce, Gd): Chondroudis, K.; Kanatzidis, M. G. *Inorg. Chem.* **1998**, *37*, 3792−3797.

(15) $A_2ThP_3Se_9$ (A = K, Rb) and $Cs_4Th_2P_5Se_{17}$: Piccoli, P. M. B.; Abney, K. D.; Schoonover, J. R.; Dorhout, P. K. *Inorg. Chem.* **2000**, *39*, 2970−2976.

(16) $K(RE)P_2Se_6$ (RE = Y, La, Ce, Pr, Gd, Tb): (a) Chen, J. H.; Dorhout, P. K. *Inorg. Chem.* **1995**, *34*, 5705−5706. (b) Chen, J. H.; Dorhout, P. K.; Ostenson, J. E. *Inorg. Chem.* **1996**, *35*, 5627−5633. (c) Orgzall, I.; Lorenz, B.; Dorhout, P. K.; Van Calcar, P. M.; Brister, K.; Sander, T.; Hochheimer, H. D. *J. Phys. Chem. Solids* **2000**, *61*, 123−134.

(17) $KLaP_2S_6$, $K_2La(P_2Q_6)_{1/2}(PQ_4)$, $K_3La(PQ_4)_2$, $K_4La_{0.67}(PQ_4)_2$, $K_{9-x}La_{1+(x/3)}(PQ_4)_4$, $KEuPQ_4$, where Q = S or Se, and $K_4Eu(PS_4)_2$: (a) Evenson, C. R. IV; Dorhout, P. K. *Inorg. Chem.* **2001**, *40*, 2884−2891. (b) Evenson, C. R. IV; Dorhout, P. K. *Inorg. Chem.* **2001**, *40*, 2875−2883.

(18) $Cs_8U_5(P_3S_{10})_2(PS_4)_6$, $K_{10}Th_3(P_2S_7)_4(PS_4)_2$, and $A_5An(PS_4)_3$, where A = K, Rb, Cs and An = U, Th: Hess, R. F.; Abney, K. D.; Burris, J. L.; Hochheimer, H. D.; Dorhout, P. K. *Inorg. Chem.* **2001**, *40*, 2851−2859.

(19) $K_3Ce(PS_4)_2$: Gauthier, G.; Jobic, S.; Brec, R.; Rouxel, J. *Inorg. Chem.* **1998**, *37*, 2332−2333. (b) $K_9Ce(PS_4)_4$: Gautheir G.; Jobic, S.; Danaire, V.; Brec, R.; Evain, M. *Acta Crystallogr.* **2000**, *C56*, E117.

(20) $Na_{1.5}Pb_{0.75}PSe_4$: Aitken, J. A.; Marking, G. A.; Evain, M.; Iordanidis, L.; Kanatzidis, M. G. *J. Solid State Chem.* **2000**, *153*, 158−169.

(21) In 1973 Hahn and Klingen studied a number of $M_2P_2Q_6$ compounds (where M = a divalent metal and Q = S or Se) and categorized them into three categories: hexagonal, monoclinic-I, and monoclinic-II. Klingen, W.; Hahn, H. *Z. Anorg. Allg. Chem.* **1973**, *396*, 271−278.

(22) Scott, B.; Pressprich, M.; Willet, R. D.; Cleary, D. A. *J. Solid State Chem* **1992**, *96*, 294−300. (b) Voroshilov, Y. V.; Vysochansky, Y. M.; Grabar, A. A.; Potorij, M. V.; Prits, I. P.; Rizak, V. M.; Sejkovskaja, L. A.; Slivka, V. Y.; Vatsenko, A. V. *Ukr. Fiz. Zh.* **1990**, *35*, 71−75.

(23) Hadenfeldt, C.; Hoedel, D. *Z. Anorg. Allg. Chem.* **1996**, *622*, 1495−1500.

(24) Yun, H.; Ibers, J. A. *Acta Crystallogr.* **1987**, *C43*, 2002−2004.

(25) Voroshilov, Y. V.; Potorii, M. N. Seikovskaya, L. A.; Yatsenko, A. V.; Prits, I. P. *Sov. Phys., Crystallogr.* **1988**, *33*, 761−762. (b) Isreal, R.; Eijt, S. W. H.; de Gelder, R.; Smits, J. M. M.; Beurskens, P. T.; Rasing, T.; van Kempen, H.; Maior, M. M.; Motrija, S. F. *Z. Kristallogr.* **1998**, *213*, 34−41.

(26) Arnautova, E.; Sviridov, E.; Rogach, E.; Savchenko, E.; Grekov, A. *Integr. Ferroelectr.* **1992**, *1*, 147−150.

(27) Penning, F. C.; Maior, M. M.; Weiegers, S. A. J.; van Kempen, H.; Maan, J. C. *Rev. Sci. Instrum.* **1996**, *67*, 2602−2605.

(28) Maxson, R. N. *Inorganic Syntheses;* Booth, H. S., Ed.; McGraw-Hill Inc.: New York, 1939; p 4.

(29) Feher, F. *Handbuch der Präparativen Anorganischen Chemie*; Brauer, G., Ed.; Ferdinand Enke: Stuttgart, Germany, 1954; Vol. 1, pp 280−281.

Se_5, and 0.177 g (2.25 mmol) Se were loaded into a fused silica tube. The tube was flame sealed under vacuum ($\sim 2 \times 10^{-4}$ mbar) and inserted in a computer controlled furnace. The tube was heated to 300 °C in 5 h and held at that temperature for 48 h. (**CAUTION:** Lanthanide metals usually react violently with chalcogens at temperatures around 300 °C.) The temperature was then raised slowly to 850 °C in 4 days and allowed to remain there for 3 days before cooling at 6 °C/hr to 250 °C; this was followed by rapid cooling to room temperature. Analysis of the products using semiquantitative energy dispersive spectroscopy (EDS) attached to a scanning electron microscope (SEM) indicated that the silver platelike crystals were $CeSe_2$,[30] and the red glassy pieces possessed various P_ySe_z compositions. Only a few yellow platelike crystals were obtained. EDS showed the presence of Na, Ce, P, and Se in these crystals. Given that we observed visual evidence of glass attack, it was assumed that the Na ions came from the fused silica tube, which contains only a few ppm of Na. After the single-crystal structure was determined and the composition revealed, we devised a rational synthesis as follows below.

II. Rational Synthesis. In a nitrogen filled glovebox, 0.070 g (0.5 mmol) Ce, 0.228 g (0.5 mmol) P_2Se_5, 0.031 g (0.25 mmol) Na_2Se, and 0.158 g (2.0 mmol) of Se were load into a graphite tube.[31] The graphite tube was inserted into a 13 mm fused silica tube and flame sealed under vacuum ($\sim 2 \times 10^{-4}$ mbar). This tube was heated from 50 to 300 °C in 5 h and kept at this temperature for 48 h. Next, the temperature was increased to 750 °C in 1 day, held there for 4 days, and cooled at a rate of 5 °C/h to 250 °C; this was followed by cooling to 50 °C in 3 h. An intimate mixture of yellow and silver platelike crystals in equal amounts was obtained after removing a small amount of excess flux with *N*,*N*-dimethylformamide (DMF). Analysis of the silver material using EDS indicated $CeSe_2$,[30] while analysis of the yellow crystals gave an average composition of $Na_{0.9}CeP_{2.1}Se_{6.2}$. The powder diffraction pattern of the bulk sample also confirmed the presence of $CeSe_2$ and $NaCeP_2Se_6$.

Preparation of $Cu_{0.4}Ce_{1.2}P_2Se_6$ and $Ce_{1.33}P_2Se_6$. In a nitrogen filled glovebox, 0.049 g (0.35 mmol) Ce, 0.011 g (0.175 mmol) Cu, 0.160 g (0.35 mmol) P_2Se_5, and 0.138 g (1.75 mmol) of Se were loaded into a graphite tube.[31] The graphite tube was inserted into a 13 mm fused silica tube, flame sealed under vacuum, and heated in the same manner as described for $NaCeP_2Se_6$ (rational synthesis). A solution of 6 parts DMF and 1 part ethylenediamine (en) was used to remove the unwanted P_ySe_z and Se, and washing with ether revealed silver polyhedra, yellow platelike crystals, and orange platelike crystals in approximately equal proportions. EDS analysis gave an average formula $Cu_3P_{1.1}Se_{4.1}$ for the silver crystals, $Cu_{0.4}Ce_{1.2}P_{2.1}Se_{6.2}$ for the yellow crystals, and $Ce_{1.3}P_{2.2}Se_{6.2}$ for the orange crystals. The majority of peaks in the powder diffraction pattern of the bulk sample could be indexed to either $Cu_{0.4}Ce_{1.2}P_2Se_6$ or $Ce_{1.33}P_2Se_6$, while the remaining peaks indicated the presence of Cu_3PSe_4.[32]

Preparation of $AgCeP_2Se_6$. In a nitrogen filled glovebox, 0.035 g (0.25 mmol) Ce, 0.027 g (0.25 mmol) Ag, 0.114 g (0.25 mmol) P_2Se_5, and 0.099 g (1.25 mmol) of Se were loaded into a graphite tube. The graphite tube was inserted into a 13 mm fused silica tube, flame sealed under vacuum, and heated in the same manner as described for $NaCeP_2Se_6$ (rational synthesis). A DMF/en solution (6:1) was used to remove the unwanted P_ySe_z and Se, and washing with ether revealed silver polyhedra and orange platelike crystals in a 60/40% mixture. Analysis of the silver polyhedra using EDS indicated the presence of $Ag_4P_2Se_6$.[33] Analysis of the orange crystals gave an average composition of $Ag_{1.1}CeP_2Se_{6.1}$. The powder diffraction pattern of the bulk sample confirmed the presence of $Ag_4P_2Se_6$[33] and $AgCeP_2Se_6$.

Physical Measurements. Powder X-ray Diffraction. Powder X-ray diffraction analyses were performed using a computer-controlled INEL CPS120 powder diffractometer with graphite monochromatized Cu Kα radiation. Powder patterns were calculated with the Cerius2 software package.[34]

Electron Microscopy. Quantitative microprobe analyses of the compounds were performed with a JEOL JSM-35C scanning electron microscope (SEM) equipped with a Tracor Northern energy dispersive spectroscopy (EDS) detector. Data were acquired with an accelerating voltage of 20 kV and a 40 s accumulation time.

Single-Crystal UV−vis. Optical transmission measurements were made at room temperature on single crystals using a Hitachi U-6000 microscopic FT spectrophotometer with an Olympus BH-2 metallurgical microscope over a range of 380−900 nm.

Raman Spectroscopy. Raman spectra were recorded on a Holoprobe raman spectrograph equipped with a 633 nm HeNe laser and a CCD camera detector. The instrument was coupled to an Olympus BX60 microscope. For each sample, crystals were simply placed onto a small glass slide, and a 50x objective lens was used to choose the area of the crystal specimens to be measured. The spot size of the laser beam when using the 50x objective lens was 10 microns.

Single-Crystal X-ray Crystallography. $NaCeP_2Se_6$. A yellow platelike crystal with dimensions of $0.09 \times 0.07 \times 0.01$ mm was mounted on a glass fiber. A Bruker SMART Platform CCD diffractometer, operating at 50 KV/40 mA and using graphite monochromatized Mo Kα radiation at −100 °C, was used for data collection. A hemisphere of data was collected in three major swaths of frames, with 0.30° steps in ω and an exposure time of 20 s per frame. Crystal stability was determined at the end of the data collection by recollecting the first 50 frames and comparing them to the original first 50 frames. No crystal decay was detected. An initial cell was obtained using the SMART[35] program, which extracted reflections from frames of the actual data collection. This matrix was used to integrate the data using the SAINT[35] program. The final cell constants were determined from a set of 4391 strong reflections obtained from data collection.

The absorption correction was done using SADABS,[35] and all refinements were carried out using the SHELXTL[35] package of crystallographic programs. The systematic absences clearly pointed to the space group $P2_1/c$. Ten atoms were located in general positions, R1 = 0.05 and wR2 = 0.13. All atoms were subsequently refined anisotropically to obtain final R1 and wR2 values of 0.0352 and 0.0895, respectively. The maximum and minimum peaks on the final difference Fourier map corresponded to 2.039 and −2.913 $e^-/Å^3$. See Table 1 for a summary of crystallographic data. A complete listing of crystallographic details is deposited as Supporting Information (CIF file).

$Cu_{0.4}Ce_{1.2}P_2Se_6$. A yellow platelike crystal with dimensions of $0.13 \times 0.09 \times 0.02$ mm was mounted on a glass fiber. The same

(30) Marcon, J. P.; Pascard, R. *Revue Internationale des Hautes Temperature et des Refractaires, Paris* **1968**, *5*, 51.
(31) A graphite tube was used in order to prevent reaction of the starting materials with the fused silica tube.
(32) Garin, J.; Parthé, E. *Acta Cryst.* **1972**, *B28*, 3672−3674. (b) Toffoli, P.; Rodier, N.; Khodadad, P. *Bull. Soc. Fr. Minéral. Cristallogr.* **1976**, *99*, 403−405.
(33) Toffoli, P.; Khodadad, P.; Rodier, N. *Acta Cryst.* **1978**, *B34*, 1779−1781.
(34) CERIUS^2, Version 3.8, Molecular Simulations Inc.: Cambridge, England, 1995.
(35) SMART, SAINT, SHELXTL V-5, SADABS, and RLATT, Bruker Analytical X-ray Instruments Inc.: Madison, WI, 1998.

Table 1. Crystallographic Data for $NaCeP_2Se_6$, $Cu_{0.4}Ce_{1.2}P_2Se_6$, and $Ce_{1.33}P_2Se_6$

empirical formula	$NaCeP_2Se_6$	$Cu_{0.4}Ce_{1.2}P_2Se_6$	$Ce_{1.33}P_2Se_6$
fw	698.81	729.26	722.06
space group	$P2_1/c$ (14)	$P2_1/c$ (14)	$P2_1/c$ (14)
a (Å)	12.1422(2)	12.041(1)	6.8057(5)
b (Å)	7.6982(1)	7.6418(8)	22.969(2)
c (Å)	11.7399(2)	11.700(1)	11.7226(8)
β (deg)	111.545(1)	111.269(2)	124.096(1)
V (Å^3)	1020.69(3)	1003.2(2)	1517.4(2)
Z	4	4	6
calcd density (g/cm^3)	4.548	4.828	4.741
μ (mm^{-1})	26.138	28.258	27.774
λ (Å)	0.71073	0.71073	0.71073
θ range for data collection (deg)	1.80−26.99	3.23−27.12	1.77 to 27.01
temp (K)	173	298	173
R indices	R1[a]= 0.0352	R1 = 0.0430	R1 = 0.0555
($I > 2\sigma(I)$)	wR2[b]= 0.0879	wR2 = 0.0968	wR2 = 0.1350
R indices	R1 = 0.0393	R1 = 0.0631	R1 = 0.0955
(all data)	wR2 = 0.0895	wR2 = 0.1022	wR2 = 0.1474
GOF on F^2	1.074	0.975	0.912

[a] $R1 = \sum||F_o| - |F_c||/\sum |F_o|$. [b] $wR2 = \{\sum [w(F_o^2 - F_c^2)^2]/\sum [w(F_o^2)^2]\}^{1/2}$.

Bruker SMART Platform CCD diffractometer that was used for the data collection of $NaCeP_2Se_6$ was used; however, in this case, it was operating at room temperature. Determination of an initial cell, data collection (40 s per frame), data processing, an absorption correction, and all refinements were performed in the same manner as for $NaCeP_2Se_6$. The final cell constants were determined from a set of 1566 strong reflections obtained from data collection.

The systematic absences indicated the space group $P2_1/c$. One cerium atom, six selenium atoms, and two phosphorus atoms were easily located in general positions, R1 = 0.14 and wR2 = 0.39. However, there remained two significant peaks in the difference Fourier map. The first peak was located approximately 3−3.5 Å from eight selenium atoms. The second peak was located about 2.2−2.5 Å from three Se atoms. The first peak was assigned as Ce(2), and the second peak was assigned as Cu(1). The R values dropped (R1 = 0.12, wR2 = 0.38); however, the isotropic displacement parameters for Ce(2) and Cu(1) were large compared to the other atoms. It was determined that Ce(2) and Cu(1) were located about 2 Å away from one another. Next, the occupancies of Ce(2) and Cu(1) were allowed to refine freely. The occupancy of Ce(2) refined to 0.19060, while the occupancy of Cu(1) reduced to 0.38628. The isotropic displacement parameters of the two atoms dropped significantly as did the R values, R1 = 0.07 and wR2 = 0.19. At this point, the formula was considered. It was determined that there was a −16 charge from the $[P_2Se_6]^{4-}$ anions, while there was a +15.82 charge from the Cu^+ and Ce^{3+} atoms (Cu^{2+} is very rare in chalcogenides). Next, the occupancies of the Cu(1) and Ce(2) atoms were constrained to a formula which would charge balance. No change in the R values was noted after least squares refinement. All atoms were subsequently refined anisotropically to obtain final R1 and wR2 values of 0.0430 and 0.1020, respectively. The maximum and minimum peaks on the final difference Fourier map corresponded to 2.160 and −1.675 e$^-$/Å^3. See Table 1 for a summary of crystallographic data. A complete listing of crystallographic details is deposited as Supporting Information (CIF file).

$Ce_{1.33}P_2Se_6$. An orange platelike crystal with dimensions of 0.25 × 0.10 × 0.03 mm was mounted on a glass fiber. The same Bruker SMART Platform CCD diffractometer that was used for the data collection of $NaCeP_2Se_6$ was used. Determination of an initial cell, data collection (30 s per frame), data processing, an absorption correction, and all refinements were performed in the same manner as for $NaCeP_2Se_6$. The final cell constants were determined from a set of 3195 strong reflections obtained from data collection.

$P2_1/c$ was chosen as the space group based upon systematic absences. Fifteen atoms were revealed in general positions within three rounds of least-squares/difference Fourier cycles (R1 = 0.12 and wR2 = 0.35). However, the isotropic displacement parameters of the three Ce atoms were very high. Therefore, the occupancies of these three atoms were allowed to refine freely. The R values dropped significantly (R1 = 0.07 and wR2 = 0.21) as did the occupancies of the three Ce atoms (Ce(1) ∼ 0.85, Ce(2) ∼ 0.31, Ce(3) ∼ 0.76). At this point, the formula was considered. It was determined that there was a −24 charge from the $[P_2Se_6]^{4-}$ anions, while there was a +23.1 charge from the Ce^{3+} atoms. Next, a constraint was added to the instruction file such that the occupancies of the Ce atoms gave a charge balanced formula. The R values were not affected by this constraint. All atoms were subsequently refined anisotropically in order to obtain final R1 = 0.0555 and wR2 = 0.1350. The maximum and minimum peaks on the final difference Fourier map corresponded to 2.316 and −2.138 e$^-$/Å^3. See Table 1 for a summary of crystallographic data. A complete listing of crystallographic details is deposited as Supporting Information (CIF file).

$AgCeP_2Se_6$. Initial data collections for $AgCeP_2Se_6$ were performed on a Bruker Smart Platform CCD diffractometer as described above. Attempts to index the cell of $AgCeP_2Se_6$ were met with great difficulty. Although the ∼7.5 Å axis was relatively easy to determine, the other two axes could not be clearly defined. Therefore, a superstructure was suspected, and several sets of data were collected. For each data collection we used a larger crystal and collected frames for longer periods of time. This resulted in the determination of larger and larger units cells. Structural models obtained from these data sets showed that the structure of $AgCeP_2Se_6$ was related to that of $NaCeP_2Se_6$, $Cu_{0.4}Ce_{1.2}P_2Se_6$, and $Ce_{1.33}P_2Se_6$; however, the refinement of these models was unsatisfactory since the R values were always above 10% and the anisotropic displacement parameters, especially those of Ag, were unacceptably large. The diffraction spots obtained from these crystals were sharp, round, and well defined; however, twinning was suspected when we noticed that many reflections were not able to be indexed to these various unit cells. In fact, these reflections could not be indexed to any cell. Viewing the reciprocal lattice using the Rlatt program[35] revealed the incommensurately modulated character of the structure. The systematic absences ($0k00$: $k = 2n+1$; $h0lm$: $l = 2n+1$) indicated $P2_1/c$ as the probable space group of the averaged structure and $P2_1/c$ ($\alpha 0 \gamma$) as the probable superspace group of the incommensurately modulated structure.

Before we discuss the data collection, structure solution, and ultimate refinement of $AgCeP_2Se_6$, it is necessary first to understand some basic concepts of aperiodic crystals and the extension of three-dimensional space crystallography to $(3 + n)$ dimensional space crystallography. For a more detailed description and a comprehensive treatment of modulated structures, see, for instance, de Wolff, Janssen et al., and van Smaalen.[36]

Superspace Description of Aperiodic Crystals. Aperiodic or quasi-periodic crystals do not possess three-dimensional translational symmetry. There are three categories of such crystals: modulated structures, intergrowth or composite materials, and quasicrystals. Although there is no translational symmetry in these materials, they

(36) de Wolff, P. M. *Acta Crystallogr.* 1974, *A30*, 777−785. (b) Janssen, T., Janner, A., Looijenga-Vos, A., de Wolff, P. M. In *International Tables for Crystallography*; Wilson, A. J. C., Ed.; Dordrecht: Kluwer Academic Publishers: 1993; Vol. C, Ch. 9.8. (c) Van Smaalen, S. *Cryst. Rev.* 1995, *4*, 79−202, and references therein.

are not disordered. Because they lack three-dimensional periodicity, aperiodic crystals cannot be adequately described using conventional three-dimensional crystallography. Therefore, it is necessary to extend the concept of a crystal to $(3 + n)$ dimensional space. X-ray diffraction of aperiodic crystals reveals sharp, well-defined diffraction spots; however, even though the strongest reflections can be indexed to an average structure with a conventional space group, a significant number of observed reflections cannot be indexed. These additional reflections are called "satellites" and must be taken into account to determine the real structure of the material. An incommensurately modulated structure, such as that of $AgCeP_2Se_6$, can be described as a perturbed periodic crystal. In this case, the atomic positions can be specified as the sum of a basic position with respect to a three-dimensional lattice and a deviation thereof. The deviation or modulation is itself periodic; however, it possesses a periodicity which is incommensurate with the three-dimensional lattice. There are two kinds of modulations which can create satellite reflections. One is a displacive modulation, in which a periodic displacement of the atomic coordinates belonging to the basic structure occurs. The other is an occupational modulation, where the atomic positions of the basic structure are occupied with a periodic probability function. Both types of modulations exist in $AgCeP_2Se_6$.

In an incommensurate $(3 + n)$ dimensional case, a structure is fully described by giving the metric and the atomic descriptions. The metric description is composed of the lattice parameters and wave vectors, q. The atoms are described by the type, position, occupancy, anisotropic displacement parameters, and modulation functions for each parameter. The concept of $(3 + n)$ dimensional crystallography has been firmly established since the 1970s but has not yet achieved main stream use because it requires an understanding of several complicated concepts, such as superspace. Nevertheless, the modulated description of some crystal structures is essential in understanding the properties of the materials.[37]

The Incommensurately Modulated Structure of $AgCeP_2Se_6$. Single crystals of $AgCeP_2Se_6$ were isolated from the batch sample and tested for quality (intensity and shape of the spots) on a Stoe image plate diffraction system (IPDS), which uses an oriented graphite (002) monochromator. An orange blocklike crystal of 0.09 × 0.08 × 0.08 mm was chosen as the best crystal for the data collection. The modulated character of the structure was obvious from the recorded frames, with satellites up to the third order clearly visible on the reconstructed frames (*ac* planes). Two data collections were, therefore, carried out in ω scan mode, with the IP at 60 mm ($\theta \leq 28°$, 6 min exposure time) for the main reflections and the first-order satellites and at 100 mm ($\theta \leq 21°$, 6 min exposure time) for all reflections up to the third order. The reflection sets were found consistent with a monoclinic symmetry and could be indexed with the following metric: $a = 6.64$, $b = 7.47$, $c = 9.95$ Å, $\beta = 92.4°$, and $q = 0.27a^* + 0.31c^*$. This cell was subsequently transformed to comply with a standard superspace group (see below), and its metric was refined with the U-fit program[38] from 903 main and first-order reflections: $a = 9.971(5)$, $b = 7.482(3)$, $c = 11.757(4)$ Å, $\beta = 145.630(9)°$, $q = 0.3121(18)a^* + 0.4116(19)c^*$, and $V = 495.1(8)$ Å^3 ($Z = 2$).

The integrated intensities were corrected for Lorentz polarization and absorption. The absorption correction was performed using a Gaussian analytical method after the crystal shape and dimensions were optimized, with the Stoe X-shape program,[39] from equivalent reflections. Both data sets were subsequently merged on the basis of common reflections, with $I/\sigma(I) > 10$. All data treatments, refinement, and Fourier syntheses were carried out with the Jana2000 program.[40] The highly redundant set of 22 362 reflections (full sphere, redundancy of 7.5) was averaged according to the $(2/m,\bar{1}1)(3 + 1)D$ point group, yielding an R_{int} value of 0.054 for observed reflections ($I \geq 3\sigma(I)$). See Table 2 for additional information.

Table 2. Crystallographic Data for $AgCeP_2Se_6$

empirical formula	$AgCeP_2Se_6$
fw	783.7
superspace group	$P2_1/c(\alpha 0 \gamma)$
a (Å)	9.971(5)
b (Å)	7.482(3)
c (Å)	11.757(4)
β (deg)	145.630
q (modulation vector)	$0.3121(18)a^* + 0.4116(19)c^*$
V (Å^3)	495.1(8)
Z	2
calcd density (g/cm^3)	5.273
μ (mm^{-1})	28.92
λ (Å)	0.71073
θ range for data collection (deg)	3.17−27.97
temp (K)	293
R^a/Rw^b for 825 main reflections	0.033/0.072
R^a/Rw^b for 1405 1st order satellites	0.046/0.090
R^a/Rw^b for 282 2nd order satellites	0.121/0.256
R^a/Rw^b for 27 3rd order satellites	0.288/0.708
R^a/Rw^b overall (2539)	0.046/0.090

[a] $R = \sum||F_o| - |F_c||/\sum |F_o|$ (for $I > 3\sigma(I)$). [b] $Rw = [\sum w(|F_o|^2 - |F_c|^2)^2/\sum w(|F_o|^4)]^{1/2}$.

The structural arrangement of the averaged structure (main reflections only) was found with SHELX direct methods.[35] All refinements were performed on F^2 using all main reflection data; however, residual factors are reported for observed reflections [$I > 3\sigma(I)$]. In the average structure, the Ag and Ce atoms were initially positioned on the same site, with a 1:1 occupancy to fulfill the $Ag^+Ce^{3+}[P^{4+}{}_2Se^{2-}{}_6]^{4-}$ charge balance. For this model, the R was 0.12, the U_{22} anisotropic displacement parameter for Ag/Ce was large, and significant residual peaks remained in the difference Fourier map. A splitting of the Ag/Ce position improved the R to ∼ 0.09 and reduced the anisotropic displacement parameters. Furthermore, the splitting caused the Ag position to be more tetrahedral-like, with shorter Ag−Se distances (ca. 2.75 Å), and that taken by Ce to be more spherical-like, with eight Se neighboring atoms (2.9−3.5 Å).

From that starting point, it was obvious that the incommensurate modulation of the $AgCeP_2Se_6$ structure implied a splitting in the internal space (phase space) of the Ag/Ce occupation and a simultaneous displacive modulation of the atomic positions. A common 3D space position and anisotropic displacement parameters were used for Ag and Ce, while modulations of the occupancy (Ag and Ce only, ensuring a full occupancy of the site through an equation) and atomic positions (all atoms) were introduced. Refinements carried out with satellite reflections up to the third order confirmed the splitting of Ag and Ce. This splitting resulted in a close to ideal tetrahedral coordination for Ag and a more spherical eight-coordinate surrounding for Ce. However, even though the splitting of the Ag and Ce positions was clear-cut, a large overshooting (>1.5) and undershooting (<−0.5) of the occupation could not be avoided.

(37) Evain, M.; Boucher, F.; Gourdon, O.; Petricek, V.; Dusek, M.; Besdicka, P. *Chem. Mater.* **1998**, *10*, 3068−3076. (b) Gourdon, O.; Hanko, J.; Boucher, F.; Petricek, V.; Whangbo, M.-H.; Kanatzidis, M. G.; Evain, M. *Inorg. Chem.* **2000**, *39*, 1398−1409.
(38) Evain, M. U-Fit program. Institut des Matériaux, Nantes, France, 1990.
(39) X-Shape program. Stoe & Cie Gmbh: Darmstadt, Germany, 1996.
(40) Petricek, V.; Dusek, M. Jana2000 program. Institute of Physics, Academy of Sciences of the Czech Republic: Prague, 1996.

Table 3. Fractional Atomic Coordinates, Center ($\hat{\chi}_4$) and Width (Δ), and Equivalent Isotropic Displacement Parameters (Å^2) for $AgCeP_2Se_6$[a]

atom	x	y	z	($\hat{\chi}_4$)	Δ	U_{eq}
Ag	0.2820(6)	0.5577(4)	0.5299(12)	0.5238(18)	1/2	0.042(4)
Ce	0.28671(18)	0.6106(2)	0.5411(2)	0.0299	1/2	0.015(2)
P	0.3732(3)	0.1072(2)	0.4367(2)			0.0137(18)
Se(1)	0.12048(14)	−0.01825(12)	0.37571(13)			0.0201(15)
Se(2)	0.60461(13)	0.30711(14)	0.67695(12)			0.0198(9)
Se(3)	0.21244(14)	0.21199(12)	0.16950(11)			0.0191(11)

[a] For an atom ν, occupation crenel function of center $\hat{x}_4^\nu$ and width Δ^ν is defined as: $p^\nu(x_4) = 1\ x_4 \lfloor \langle \hat{x}_4^\nu - \Delta^\nu/2, \hat{x}_4^\nu + \Delta^\nu/2\rangle$, $p^\nu(x_4) = 0\ x_4 \lceil \langle \hat{x}_4^\nu - \Delta^\nu/2, \hat{x}_4^\nu + \Delta^\nu/2\rangle$.

To get a proper splitting of the Ag/Ce occupation, a built-in crenel function[41−43] was used, which considerably improved the agreement. With the inclusion of new waves (on the positions up to the 2nd order for Ag, Ce, and P, the 3rd order for Se, and on the anisotropic displacement parameters up to the 1st order for Ag, Ce, and Se atoms) and a secondary extinction coefficient,[44] the overall residual factor converged at the final stage to R = 0.046 and Rw = 0.090 for 2539 reflections and 207 parameters. The maximum and minimum peaks on the final difference Fourier map corresponded to 3.9 and −2.5 e$^-$/Å^3. See Table 2 for the *R* values for each set of reflections. Other essential results for this model are gathered in Table 3. Since two rather short Ag−Se distances occur near the crenel edge (see structure description), several attempts were made to homogenize the Ag−Se distances over the full crenel width by means of more complicated models, including saw-tooth functions and/or multi-crenel functions for both Ag and Se atoms. Apart from increasing the number of parameters for an equivalent residual factor, these attempts could not suppress the two short Ag−Se distances. A complete listing of crystallographic details are deposited as Supporting Information (CIF file).

Results and Discussion

Synthesis. Unlike previous reports from our laboratory, flux chemistry was not employed in this work. Our initial goal to synthesize $CePSe_4$ via stoichiometric reactions, as an analogue of the $LnPS_4$ family, was not achieved; instead, we observed that in several Ce/P_2Se_5/Se reaction mixtures, significant attack of the silica tubes occurred to abstract sodium atoms to form $NaCeP_2Se_6$. After this serendipitous synthesis, we performed several sets of reactions in the Ce/P_2Se_5/Na_2Se/Se system. Since $NaCeP_2Se_6$ forms by scavenging traces of sodium, we recognized that this structure type is extremely stable and set out to prepare substitutional Cu and Ag analogues. These investigations led to the discovery of $Cu_{0.4}Ce_{1.2}P_2Se_6$, $AgCeP_2Se_6$, and $Ce_{1.33}P_2Se_6$, which possess related structure types.

$NaCeP_2Se_6$, $Cu_{0.4}Ce_{1.2}P_2Se_6$, and $AgCeP_2Se_6$ were synthesized from nearly stoichiometric proportions of the elements plus some extra selenium at temperatures in the range of 750−850 °C. Attempts to prepare the compounds in pure form by varying several reaction parameters were not successful. Increasing the ratio of Ce from 1 to 2 equiv favored the formation of $CeSe_2$[30] in the Na system. In the Cu and Ag systems, this change resulted only in $Ag_4P_2Se_6$[33] or Cu_3PSe_4,[32] and $CeSe_2$ and did not lead to quaternary compounds. Additional amounts of Na_2Se in the Na system also promoted $CeSe_2$. Reactions rich in Ag or Cu in the Ag−Ce−P−Se or Cu−Ce−P−Se systems gave markedly larger amounts of $Ag_4P_2Se_6$ and Cu_3PSe_4. Added quantities of P_2Se_5 made reaction isolations more difficult and also aided the formation of $CeSe_2$. Extra Se in all three systems yielded products rich in $CeSe_2$ as well. For example, when the ratio of Se was raised to 10 equiv, no quaternary products were found. Lesser amounts of Se in all systems led to poorly melted reaction mixtures. Likewise, lower reaction temperatures also gave insufficient melting.

$Ce_{1.33}P_2Se_6$ was found in the same reaction that produced $Cu_{0.4}Ce_{1.2}P_2Se_6$. Since Raman and band gap measurements were performed on single crystals (which were subsequently taken to the SEM for EDS analysis), there were no problems with the characterization of these two phases. Oddly, attempts to synthesize this compound in the ternary system were met with difficulty, although a number of reaction mixtures produced a small amount of this phase. For example, the reaction of Ce/P_2Se_5/Se in a 1:2:6 molar ratio produced several orange crystals of $Ce_{1.33}P_2Se_6$, but not nearly as much as was found in the Ce/P_2Se_5/Cu/Se system reaction. These reactions rich in P_2Se_5 and Se were also very hard to work up since they also produced large amounts of glassy P_ySe_z. Reactions that were closer to the $Ce_{1.33}P_2Se_6$ stoichiometry produced large amounts of a new ternary phase that we have not yet been able to fully characterize.[45]

We rationalize the failure to synthesize selenium analogues of $LnPS_4$ by the tendency of phosphorus to acquire an oxidation state of 4+ rather than 5+ in a selenide environment under the conditions employed. This is supported by the many more selenophosphates containing the $[P_2Se_6]^{4-}$ unit than those containing the $[PSe_4]^{3-}$ unit, which suggests that P^{4+} is preferred over P^{5+} in the selenium systems.

(41) Petricek, V.; van de Lee, A.; Evain, M. *Acta Crystallogr.* **1995**, *A51*, 529−535.
(42) Boucher, F.; Evain, M.; Petricek, V. *Acta Crystallogr.* **1996**, *B52*, 100−109.
(43) A crenel function is preferable to the Fourier series in many respects. First, it considerably reduces the number of parameters. Only two parameters are required to describe an occupation crenel function for an atom ν, the crenel width (Δ^ν), and the crenel midpoint ($\hat{x}_4^\nu$). Second, it avoids nonphysical occupation probabilities. Finally, it prevents intermediate situations produced by the Fourier series expansion at the crenel-like "steps". In the present case, the intermediate situation would be the simultaneous presence of Ag and Ce. In this situation an orthogonalization procedure is usually necessary to reduce correlations. Indeed, with the application of crenel functions, the modulation functions are not defined for all $\hat{x}_4^\nu$ values and thus the orthogonality condition is not fulfilled for the set of harmonic functions.
(44) Becker, P. J.; Coppens, P. *Acta Crystallogr.* **1974**, *A30*, 129.
(45) The powder X-ray diffraction pattern of this ternary phase was similar to that of $CeSe_2$, suggesting it may be $CeSe_{2-x}P_y$. Energy dispersive spectroscopy indicated at least 10 atomic % of P in this phase.

Table 4. Selected Distances (Å) and Angles (deg) for $NaCeP_2Se_6$ and $Cu_{0.4}Ce_{1.2}P_2Se_6$

distances	$NaCeP_2Se_6$	distances	$Cu_{0.4}Ce_{1.2}P_2Se_6$	angles	$NaCeP_2Se_6$	angles	$Cu_{0.4}Ce_{1.2}P_2Se_6$
Ce−Se(2)	3.0674(8)	Ce(1)−Se(2)	3.060(1)	Se(4)−Ce−Se(5)	74.49(2)	Se(4)−Ce(1)−Se(5)	74.75(3)
Ce−Se(3)	3.0773(8)	Ce(1)−Se(3)	3.063(1)	Se(3)−Ce−Se(6)	76.79(2)	Se(3)−Ce(1)−Se(6)	75.63(3)
Ce−Se(4)	3.1078(8)	Ce(1)−Se(5)	3.090(1)	Se(2)−Ce−Se(4)	80.10(2)	Se(2)−Ce(1)−Se(4)	77.91(3)
Ce−Se(5)	3.1112(8)	Ce(1)−Se(4)	3.092(1)	Se(2)−Ce−Se(5)	80.76(2)	Se(2)−Ce(1)−Se(5)	80.99(3)
Ce−Se(5)	3.1393(8)	Ce(1)−Se(5)	3.109(1)	Se(3)−Ce−Se(5)	86.30(2)	Se(3)−Ce(1)−Se(5)	87.31(3)
Ce−Se(6)	3.1855(8)	Ce(1)−Se(6)	3.174(1)	Se(5)−Ce−Se(6)	87.81(2)	Se(5)−Ce(1)−Se(6)	89.23(3)
Ce−Se(6)	3.2365(8)	Ce(1)−Se(6)	3.227(1)	Se(1)−Ce−Se(4)	115.78(2)	Se(1)−Ce(1)−Se(4)	114.82(3)
Ce−Se(4)	3.3344(8)	Ce(1)−Se(4)	3.345(1)	Se(4)−Ce−Se(6)	119.25(2)	Se(4)−Ce(1)−Se(6)	120.76(3)
Ce−Se(1)	3.4733(9)	Ce(1)−Se(1)	3.647(1)	Se(1)−Ce−Se(6)	124.15(2)	Se(1)−Ce(1)−Se(6)	123.75(3)
Na−Se(4)	3.097(3)	Ce(2)−Se(3)	2.955(4)	Se(1)−Na−Se(3)	68.65(7)	Se(1)−Ce(2)−Se(3)	72.81(9)
Na−Se(3)	3.099(3)	Ce(2)−Se(1)	2.996(4)	Se(3)−Na−Se(6)	73.35(7)	Se(3)−Ce(2)−Se(6)	75.23(9)
Na−Se(1)	3.102(3)	Ce(2)−Se(4)	3.063(4)	Se(1)−Na−Se(6)	74.22(7)	Se(2)−Ce(2)−Se(4)	75.42(8)
Na−Se(1)	3.110(3)	Ce(2)−Se(1)	3.080(4)	Se(2)−Na−Se(4)	76.78(7)	Se(1)−Ce(2)−Se(6)	77.38(9)
Na−Se(2)	3.297(3)	Ce(2)−Se(2)	3.255(4)	Se(1)−Na−Se(2)	94.76(8)	Se(1)−Ce(2)−Se(2)	91.4(1)
Na−Se(3)	3.380(3)	Ce(2)−Se(6)	3.296(4)	Se(1)−Na−Se(4)	99.04(9)	Se(1)−Ce(2)−Se(4)	93.9(1)
Na−Se(6)	3.403(3)	Ce(2)−Se(2)	3.448(4)	Se(2)−Na−Se(3)	129.4(1)	Se(2)−Ce(2)−Se(3)	128.08(11)
Na−Se(2)	3.501(3)	Ce(2)−Se(3)	3.449(4)			Se(1)−Cu−Se(3)	114.0(2)
		Ce(2)−Cu	2.052(6)			Se(1)−Cu−Se(3)	116.0(2)
		Cu−Se(1)	2.258(4)			Se(1)−Cu−Se(1)	129.8(2)
		Cu−Se(3)	2.374(4)	Se(4)−P(1)−P(2)	103.65(9)	Se(1)−P(1)−P(2)	103.0(1)
		Cu−Se(1)	2.455(4)	Se(1)−P(1)−P(2)	104.73(9)	Se(4)−P(1)−P(2)	104.1(1)
P(1)−P(2)	2.230(3)	P(1)−P(2)	2.231(4)	Se(2)−P(1)−P(2)	105.83(9)	Se(2)−P(1)−P(2)	106.0(1)
P(1)−Se(1)	2.167(2)	P(1)−Se(2)	2.169(3)	Se(2)−P(1)−Se(4)	107.29(8)	Se(2)−P(1)−Se(4)	108.5(1)
P(1)−Se(2)	2.186(2)	P(1)−Se(4)	2.176(3)	Se(1)−P(1)−Se(4)	112.62(8)	Se(1)−P(1)−Se(4)	114.1(1)
P(1)−Se(4)	2.194(2)	P(1)−Se(1)	2.186(3)	Se(1)−P(1)−Se(2)	121.08(9)	Se(1)−P(1)−Se(2)	119.5(1)
P(2)−Se(3)	2.177(2)	P(2)−Se(3)	2.175(3)	Se(3)−P(2)−P(1)	103.08(9)	Se(3)−P(2)−P(1)	103.0(1)
P(2)−Se(6)	2.203(2)	P(2)−Se(6)	2.193(3)	Se(5)−P(2)−P(1)	105.05(9)	Se(5)−P(2)−P(1)	105.2(1)
P(2)−Se(5)	2.214(2)	P(2)−Se(5)	2.204(3)	Se(6)−P(2)−P(1)	108.51(9)	Se(6)−P(2)−P(1)	109.0(1)
				Se(5)−P(2)−P(6)	110.69(8)	Se(5)−P(2)−P(6)	111.0(1)
				Se(3)−P(2)−P(6)	112.57(8)	Se(3)−P(2)−P(6)	113.1(1)
				Se(3)−P(2)−P(5)	116.10(8)	Se(3)−P(2)−P(5)	114.8(1)

Perhaps the use of lithium containing selenophosphate fluxes will prove more useful in meeting the synthetic challenge of stabilizing $LnPSe_4$ compounds.

Structure. $NaCeP_2Se_6$ is isostructural to the $KLnP_2Q_6$ family of compounds, where Ln = La, Ce, Pr for Q = Se[16] and Ln = La for Q = S.[17] The structure consists of $[CeP_2Se_6]_n^{n-}$ slabs separated by Na^+ cations, see Figure 1. The Na atoms are not located in the middle of the interlayer space but instead are nestled into holes present in the layers. The coordination environment of the Na atoms can be best described as a highly distorted square antiprism or bicapped trigonal prism. The Na−Se distances range from 3.097(3) to 3.501(3) Å, see Table 4. Each layer of $[CeP_2Se_6]_n^{n-}$ consists of $CeSe_9$ distorted tricapped trigonal-prisms and $[P_2Se_6]^{4-}$ ethane-like ligands. The nine Ce−Se distances range from 3.0674(8) to 3.4733(9) Å, see Table 4. The Ce and Se atoms alone form a two-dimensional network. Each $CeSe_9$ connects to five others by sharing an edge with one other $CeSe_9$ and corners with four other $CeSe_9$ polyhedra. Each $[P_2Se_6]^{4-}$ anion connects to four $CeSe_9$ units by sharing faces with two $CeSe_9$, an edge with another $CeSe_9$, and a corner with a fourth $CeSe_9$, see Figure 2.

According to Dorhout et al., one can derive the $KLnP_2Q_6$ structure from that of $Fe_2P_2S_6$[46] (monoclinic-I, $M^{II}PQ_3$ structure type[21]) by taking two $Fe_2P_2S_6$ layers and condensing them together into a bilayer while removing half of the metal atoms.[16b] The metal coordination sphere expands and the $[P_2Se_6]^{4-}$ ligands twist during this condensation. Figure 3a shows a layer of $Fe_2P_2S_6$. Figure 3b shows the bilayered structure of $NaCeP_2Se_6$ broken down into monolayers. Within each monolayer the Ce atoms have a coordination number of seven. Looking at the large holes in these layers, it is easy to understand why the Na atoms are nestled into them rather than into the interlayer space, see Figure 3c. Conden-

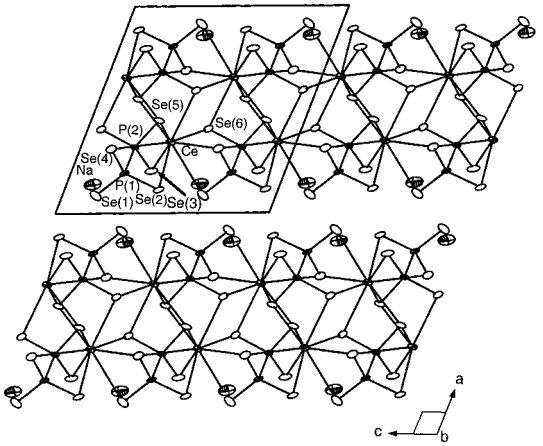

Figure 1. ORTEP representation of $NaCeP_2Se_6$ viewed down the *b* axis with thermal vibrational (95%) ellipsoids.

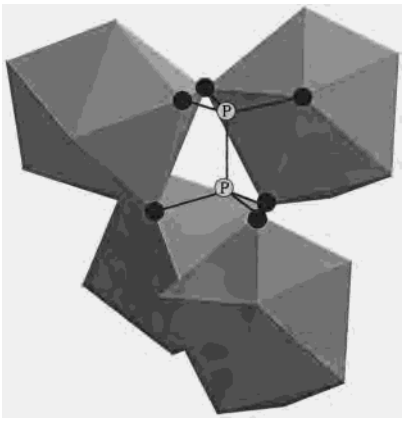

Figure 2. The binding mode of the $[P_2Se_6]^{4-}$ anion in $NaCeP_2Se_6$. The $[P_2Se_6]^{4-}$ unit connects to four $CeSe_9$ polyhedra by sharing faces with two $CeSe_9$, an edge with another $CeSe_9$, and a corner with a fourth $CeSe_9$.

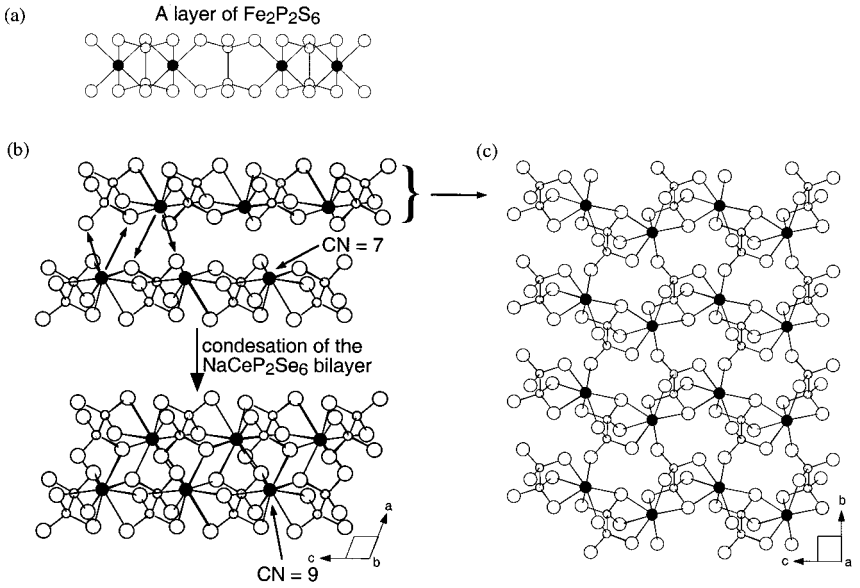

Figure 3. (a) One layer of $Fe_2P_2S_6$ (monoclinic-I, $M^{II}PQ_3$ structure type) viewed down the *a* axis. Removal of half the metal atoms in this layer, in combination with a twisting of the $[P_2S_6]^{4-}$ units, creates an "MP_2S_6" layer similar to that found in $NaCeP_2Se_6$. (b) In $NaCeP_2Se_6$, two layers of "CeP_2Se_6", which contain seven-coordinate Ce atoms, condense side-by-side via cross-layer Ce−Se bonds in order to create a bilayered structure and expand the Ce coordination number to nine. (c) A single "CeP_2Se_6" layer viewed down the *a* axis.

sation of these monolayers into a bilayer expands the Ce atom coordination number to nine. The lamellar $KBiP_2Se_6$ and $KSbP_2Se_6$[47] have structures which are are also similar to the structure of the $KLnP_2Q_6$ family. In these compounds, the monolayers contain five-coordinate Bi or Sb atoms. The association of two single layers gives rise to a bilayered structure in which the metal coordination is expanded to a distorted octahedron.

A simpler and more concise relationship between $NaCeP_2Se_6$ and the members of the $KLnP_2Q_6$ family can be drawn to the monoclinic-II, $M^{II}PQ_3$ structure type ($Pb_2P_2S_6$,[22] $Pb_2P_2Se_6$,[24] $Sn_2P_2S_6$[22] (one of three allotropes), $Sn_2P_2Se_6$[25] (one of two allotropes), $Sr_2P_2S_6$,[23] $Ca_2P_2S_6$,[23] and $Ba_2P_2Se_6$[48]). Phases belonging to the monoclinic-II structure type have three-dimensional frameworks, with lattice parameters similar to those reported here and to the $KLnP_2Q_6$ family. Furthermore, compounds of the monoclinic-II structure type adopt the same space group as those reported here, $P2_1/c$, and, therefore, better resemble the $[P_2Se_6]^{4-}$ arrangement observed in these structures, see Figure 4. A simple substitution of the 2^+ metal by a 1^+ metal and 3^+ metal in an AABB fashion takes place in order to create a layered structure with a doubling of the *a* axis. The metal coordination sphere in the monoclinic-II structure (CN = 8−9) is similar to that found in the new selenophosphates reported here.

The structure of $Cu_{0.4}Ce_{1.2}P_2Se_6$ is similar to that of $NaCeP_2Se_6$; however, it is three dimensional because the Ce(2) and Cu(1) atoms take the place of the alkali cations and connect the layers, Figure 5. Atom Ce(1) is eight-coordinate and resides in a distorted bicapped trigonal prism. These eight

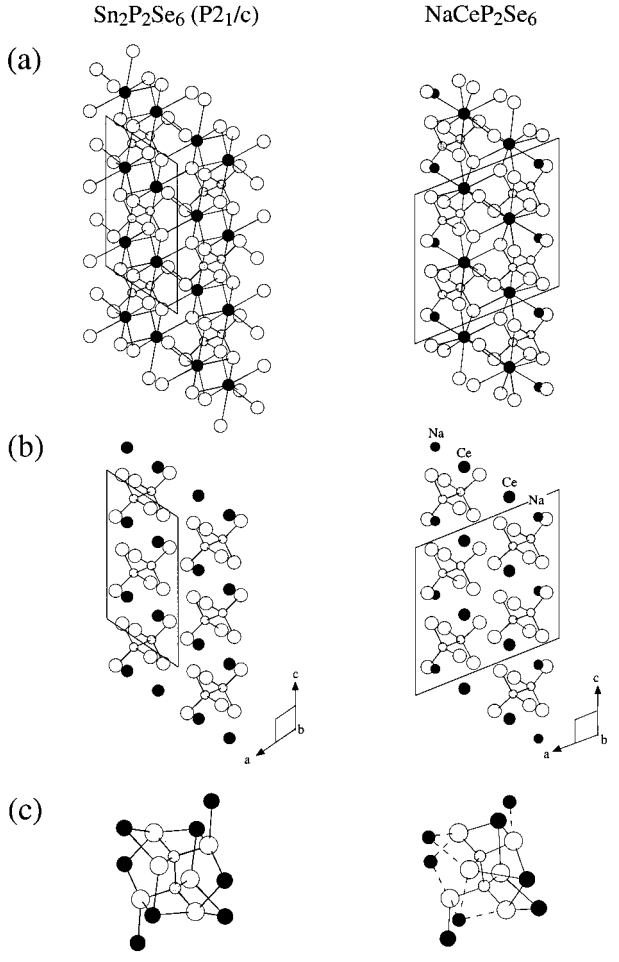

Figure 4. A comparison of the structure of $Sn_2P_2Se_6$ (monoclinic-II, $M^{II}PQ_3$ structure type) to that of $NaCeP_2Se_6$. (a) Both structures viewed down the *b* axis. (b) Removal of all Sn−Se and Ce−Se bonds shows more clearly the arrangement of the $[P_2Se_6]^{4-}$ ligands in these two structures. (c) The binding mode of the $[P_2Se_6]^{4-}$ ligand in each structure. Dashed bonds are used to show Na- - -Se interactions.

(46) Klingen, W.; Eulenberger, G.; Hahn, H. *Z. Anorg. Allg. Chem.* **1973**, *101*, 97−112.
(47) McCarthy, T. J.; Kanatzidis, M. G. *J. Chem. Soc., Chem. Commun.* **1994**, 1089−1090.
(48) Chondroudis, K.; Kanatzidis, M. G. unpublished results.

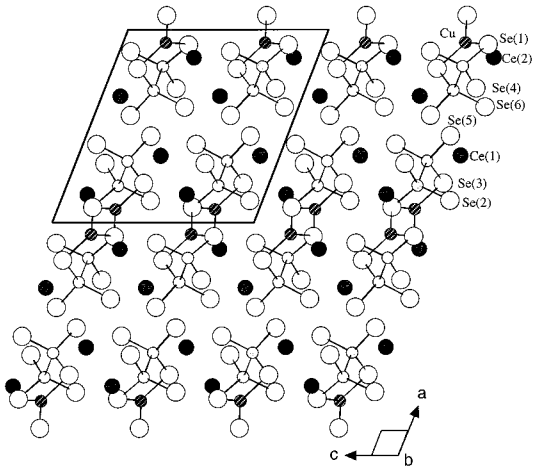

Figure 5. The structure of $Cu_{0.4}Ce_{1.2}P_2Se_6$ viewed down the *b* axis.

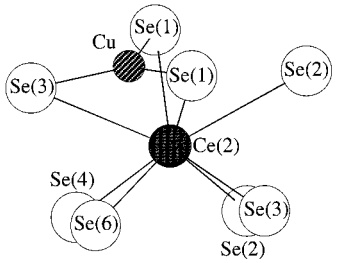

Figure 6. The coordination sphere of the Cu(1)/Ce(2) site in $Cu_{0.4}Ce_{1.2}P_2Se_6$. This pocket is ~40% occupied by Cu and ~20% occupied by Ce. The remaining 40% is vacant. The Cu(1)−Ce(2) distance is 2.052(6) Å.

Ce−Se distances range from 3.060(1) to 3.345(2) Å, see Table 4. The ninth Se atom is too far to be considered bonding, 3.648(2) Å. The Ce(2) atom (40% occupied) also resides in a distorted bicapped trigonal prism of selenium atoms (Figure 6) and occupies a position in the vicinity of the Na atom in $NaCeP_2Se_6$. The copper position (20% occupied) adopts a trigonal planar geometry and lies in what was formerly the interlayer space. The Cu−Se distances are 2.258(4), 2.374(4), and 2.455(4) Å. The Cu−Ce(2) nonbonding distance is 2.052(6) Å; however, these atoms do not reside in this pocket at the same time, Figure 6. Furthermore, this pocket remains vacant 40% of the time.

$Ce_{1.33}P_2Se_6$, which can also be expressed as $Ce_4(P_2Se_6)_3$, adopts a three-dimensional structure, which is also related to the structures described above, but is more closely related to the monoclinic-II, $M^{II}PQ_3$ structure type, see Figure 7. In this case, the 2+ metal is substituted by Ce^{3+} and vacancies. There are three crystallographically unique Ce atoms in the structure which are partially occupied. These three Ce atoms cause the *b* axis to be three-fold that of the monoclinic-II, $M^{II}PQ_3$ structure type, whereas the *a* and *c* axes are quite similar. All three Ce atoms lie within a distorted bicapped trigonal prism of Se atoms. The Ce−Se distances dictate the occupancies of the Ce sites, where the more spherical the site the more heavily it is occupied. In the case of Ce(1), the Ce−Se distances have the largest distribution, 3.022(4)−3.408(4) Å; therefore, Ce(1) is occupied the least, 0.345(3), and has the largest anisotropic displacement parameter. The Ce−Se distances for Ce(3) have the smallest range, 3.060(2)−3.263(2) Å; consequently, Ce(3) is occupied the most, 0.875(3). Ce(2) falls between Ce(1) and Ce(3) in terms of Ce−Se distances, 3.055(2)−3.319(2) Å, and the corresponding occupancy, 0.778(2). Table 5 lists selected bond distances and angles for $Ce_{1.33}P_2Se_6$.

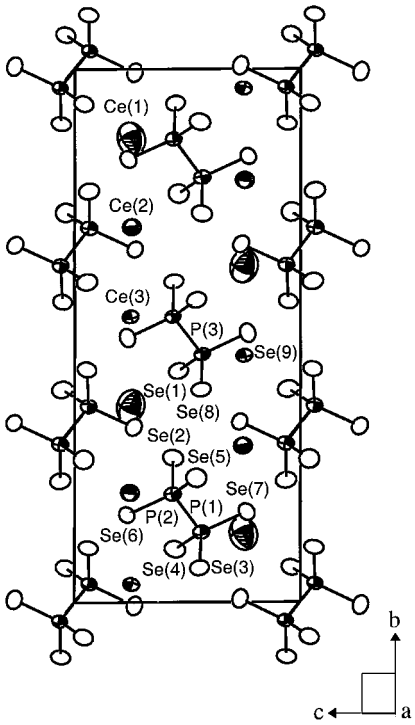

Figure 7. ORTEP representation of $Ce_{1.33}P_2Se_6$ viewed down the *a* axis with thermal vibrational (95%) ellipsoids. Each of the three Ce sites is partially occupied.

In the literature there exists several other phases with stoichiometries similar to that of $Ce_{1.33}P_2Se_6$ ($Ce_4(P_2Se_6)_3$), namely, $In_4(P_2S_6)_3$,[49] $In_4(P_2Se_6)_3$,[49,50] α-[51] and β-$Bi_4(P_2Se_6)_3$,[52] and $Sb_4(P_2Se_6)_3$.[51] $In_4(P_2S_6)_3$ is related to $Fe_2P_2S_6$ (monoclinic-I, $M^{II}PQ_3$ structure type), however, the *c* axis is tripled and the space group is of a lower symmetry. $In_4(P_2Se_6)_3$ is related to $Fe_2P_2Se_6$[46] (hexagonal, $M^{II}PQ_3$ structure type).[21] Although a hexagonal symmetry was initially determined where the M site was 2/3 occupied by In, an orthorhombic structure was later established, with an ordering of the metal vacancies, describing $In_4(P_2Se_6)_3$ as build from a six-fold superstructure of $Fe_2P_2Se_6$. α-$Bi_4(P_2Se_6)_3$ and $Sb_4(P_2Se_6)_3$ have a remarkable relationship with the monoclinic-II, $M^{II}PQ_3$ structure type. This structure possesses cuts of the $M^{II}PQ_3$ structure separated by sections of a new type. The breakdown of the monoclinic-II, $M^{II}PQ_3$ structure type probably results from the fact that Sb and Bi can tolerate a lower coordination number than eight and a highly unsymmetrical coordination sphere. β-$Bi_4(P_2Se_6)_3$ represents a novel, complicated structure that possesses a unique arrangement of the $[P_2Se_6]^{4-}$ units.

Interestingly, two members of the monoclinic-II, $M^{II}PQ_3$ structure type, namely $Sn_2P_2S_6$ and $Sn_2P_2Se_6$, undergo a phase

(49) Diehl, R.; Carpentier, C. *Acta Crystallogr.* **1978**, *B34*, 1097−1105.
(50) Katty, A.; Soled, S.; Wold, A. *Mater. Res. Bull.* **1977**, *12*, 663−666.
(51) Ruck, M. *Z. Anorg. Allg.Chem.* **1995**, *621*, 1344−1350.
(52) Aitken, J. A.; Brown, S.; Chondroudis, K.; Jobic, S.; Brec, R.; Kanatzidis, M. G. *Inorg. Chem.* **1964**, *38*, 4795−4800.

Table 5. Selected Distances (Å) and Angles (deg) for $Ce_{1.33}P_2Se_6$

distances		angles	
Ce(1)−Se(2)	3.022(4)	Se(3)−Ce(1)−Se(9)	74.09(9)
Ce(1)−Se(7)	3.027(4)	Se(2)−Ce(1)−Se(5)	76.5(1)
Ce(1)−Se(9)	3.055(4)	Se(1)−Ce(1)−Se(3)	76.88(9)
Ce(1)−Se(3)	3.115(4)	Se(1)−Ce(1)−Se(9)	79.49(9)
Ce(1)−Se(5)	3.210(4)	Se(2)−Ce(1)−Se(7)	90.3(1)
Ce(1)−Se(1)	3.230(4)	Se(5)−Ce(1)−Se(7)	92.1(1)
Ce(1)−Se(8)	3.375(4)	Se(4)−Ce(1)−Se(8)	123.4(1)
Ce(1)−Se(4)	3.408(4)		
Ce(2)−Se(7)	3.055(2)	Se(4)−Ce(2)−Se(8)	72.28(4)
Ce(2)−Se(2)	3.083(2)	Se(2)−Ce(2)−Se(7)	75.90(4)
Ce(2)−Se(6)	3.112(2)	Se(2)−Ce(2)−Se(5)	76.40(4)
Ce(2)−Se(8)	3.117(2)	Se(5)−Ce(2)−Se(7)	81.90(4)
Ce(2)−Se(5)	3.163(2)	Se(6)−Ce(2)−Se(8)	89.57(4)
Ce(2)−Se(4)	3.222(2)	Se(4)−Ce(2)−Se(6)	91.70(4)
Ce(2)−Se(5)	3.283(2)	Se(2)−Ce(2)−Se(5)	124.77(5)
Ce(2)−Se(2)	3.319(2)		
Ce(3)−Se(9)	3.060(2)	Se(6)−Ce(3)−Se(8)	73.10(4)
Ce(3)−Se(6)	3.099(2)	Se(4)−Ce(3)−Se(8)	73.78(4)
Ce(3)−Se(3)	3.108(2)	Se(1)−Ce(3)−Se(3)	76.93(4)
Ce(3)−Se(8)	3.108(2)	Se(4)−Ce(3)−Se(6)	78.84(4)
Ce(3)−Se(4)	3.121(2)	Se(3)−Ce(3)−Se(9)	91.13(4)
Ce(3)−Se(1)	3.232(2)	Se(1)−Ce(3)−Se(9)	92.84(4)
Ce(3)−Se(1)	3.258(2)	Se(1)−Ce(3)−Se(3)	124.29(4)
Ce(3)−Se(3)	3.263(2)		
P(1)−P(3)	2.230(5)	Se(3)−P(1)−P(3)	102.4(2)
P(1)−Se(7)	2.185(3)	Se(4)−P(1)−P(3)	106.0(2)
P(1)−Se(3)	2.195(4)	Se(7)−P(1)−P(3)	106.0(2)
P(1)−Se(4)	2.207(3)	Se(3)−P(1)−Se(4)	107.9(2)
P(3)−Se(2)	2.182(4)	Se(4)−P(1)−Se(7)	115.8(2)
P(3)−Se(5)	2.186(4)	Se(3)−P(1)−Se(7)	117.3(1)
P(3)−Se(6)	2.213(4)	Se(2)−P(3)−P(1)	104.0(2)
		Se(6)−P(3)−P(1)	105.3(2)
		Se(5)−P(3)−P(1)	107.8(2)
		Se(2)−P(3)−Se(5)	110.3(2)
		Se(5)−P(3)−Se(6)	113.4(2)
		Se(2)−P(3)−Se(6)	115.2(2)
P(2)−P(2)	2.232(6)	Se(8)−P(2)−P(2)	102.5(2)
P(2)−Se(8)	2.193(4)	Se(9)−P(2)−P(2)	105.2(2)
P(2)−Se(9)	2.196(4)	Se(1)−P(2)−P(2)	107.1(2)
P(2)−Se(1)	2.203(3)	Se(1)−P(2)−Se(8)	110.7(1)
		Se(1)−P(2)−Se(9)	114.2(2)
		Se(8)−P(2)−Se(9)	115.8(1)

transition from the centrosymmetric $P2_1/c$ structure to that of *Pc* at low temperatures.[25b,53] The *Pc* structure shows strong ferroelectric behavior.[26] With this in mind, we solved both $NaCeP_2Se_6$ and $Ce_{1.33}P_2Se_6$ in the space group *Pc* since their single-crystal data were collected at low temperature. $NaCeP_2Se_6$ could be refined in *Pc* with R1 = 0.0310, wR2 = 0.0767 [$I > 2\sigma(I)$], and a Flack parameter of 0.45(7). Anisotropic refinement of the atoms caused nearly all to become nonpositive definite. $Ce_{1.33}P_2Se_6$ could be refined in the space group *Pc* with R1 = 0.0610, wR2 = 0.1532 [$I > 2\sigma(I)$], and a Flack parameter of 0.43(7). Anisotropic refinement of the atoms in this case lead to 1/3 of the atoms being nonpositive definite. Therefore, we prefer the better behaving solutions in $P2_1/c$ and, consequently, the centrosymmetric description above (at least above −100 °C).

Incommensurate Structure of $AgCeP_2Se_6$. $AgCeP_2Se_6$ represents an incommensurately modulated version of the structures described above. The basic structure (0th order of the real modulated structure) is similar to that of $NaCeP_2Se_6$, $Cu_{0.4}Ce_{1.2}P_2Se_6$, and $Ce_{1.33}P_2Se_6$. The ethane-like $[P_2Se_6]^{4-}$ groups are bonded to the Ag and Ce cations to form a three-dimensional structure. The Ce cations are linked to four such

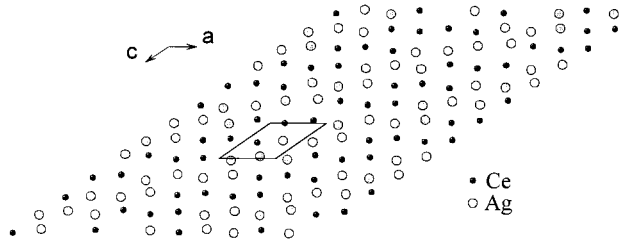

Figure 8. Illustration of the Ag/Ce distribution in the *ac* plane of $AgCeP_2Se_6$, resulting from the occupational and positional modulations.

$[P_2Se_6]^{4-}$ entities via one, two, or three Se atoms. The Ag cations are displaced from the Ce locations to favor four shorter bonds with Se atoms of three different $[P_2Se_6]^{4-}$ groups, thus realizing a more common lower coordination.[54]

In the real, modulated structure, the coordination difference between Ag and Ce is realized through (i) a segregation of the cations in ribbons along the *ac* plane (see Figure 8) and (ii) heavy displacive modulations both of the cations and anions. Although the anisotropic displacive modulations are large (see for instance that of Se(2) in Figure 9a), the $[P_2Se_6]^{4-}$ group geometry is preserved as shown in the P−Se and P−P distances, see Figure 9b. The average P−P distance is 2.23 Å, and the average P−Se distances are 2.19, 2.19, and 2.18 Å for Se(1), Se(2), and Se(3), respectively, in agreement with the literature.[14,16,47,55] The Ag−Se distances show a preferential four-fold coordination with a tendency for a two-fold coordination near the crenel edge ($t \approx 0.45$), see Figure 9c. This two-fold coordination should be cautiously considered since it may be an artifact of the refinement (although it was always associated with good residual values whatever the refinement model used). Indeed, it is clear that the shortest Ag−Se distance arises when a Se atom abruptly enters the coordination sphere of Ag. This Ag−Se distance swiftly shifts from over 4 Å for $t \approx 0.35$ to ca. 2.8 Å for $t \approx 0.4$, which is probably not properly described by a continuous function, thus the border effect. The Ce−Se distance evolution shows a coordination close to that found in the average cell, see Figure 9c.

Spectroscopy. The transparent, well-formed crystals of yellow $NaCeP_2Se_6$, yellow $Cu_{0.4}Ce_{1.2}P_2Se_6$, and orange $Ce_{1.33}P_2Se_6$ were suitable for single-crystal optical transmission measurements. The compounds exhibit sharp optical absorptions of 2.37, 2.24, and 1.94 eV respectively, consistent with their yellow to orange colors, see Figure 10. As expected, there is a clear trend observed in these three materials, where increasing amounts of Ce lower the resulting band gap. The shape of the absorption edge in these spectra can be analyzed to distinguish between a direct and an indirect gap semiconductor.[56] In semiconductors, the energy dependence of the absorption coefficient is quadratic in materials with a direct energy gap, whereas in those with indirect gaps, the dependence scales to the square root.[57] Data plots of (absorption)^2 versus energy and (absorption)$^{(1/2)}$

(53) Dittmar, G.; Schäfer, H. *Z. Naturforsh.* **1974**, *29b*, 312−317.

(54) Gaudin, E.; Boucher, F.; Evain, M. *J. Solid State Chem.*, in press.

(55) McCarthy, T. J.; Kanatzidis, M. G. *Inorg. Chem.* **1995**, *34*, 1257−1267.

(56) This type of analysis is only valid if single-crystal spectra are available. It is less reliable when using diffuse reflectance data.

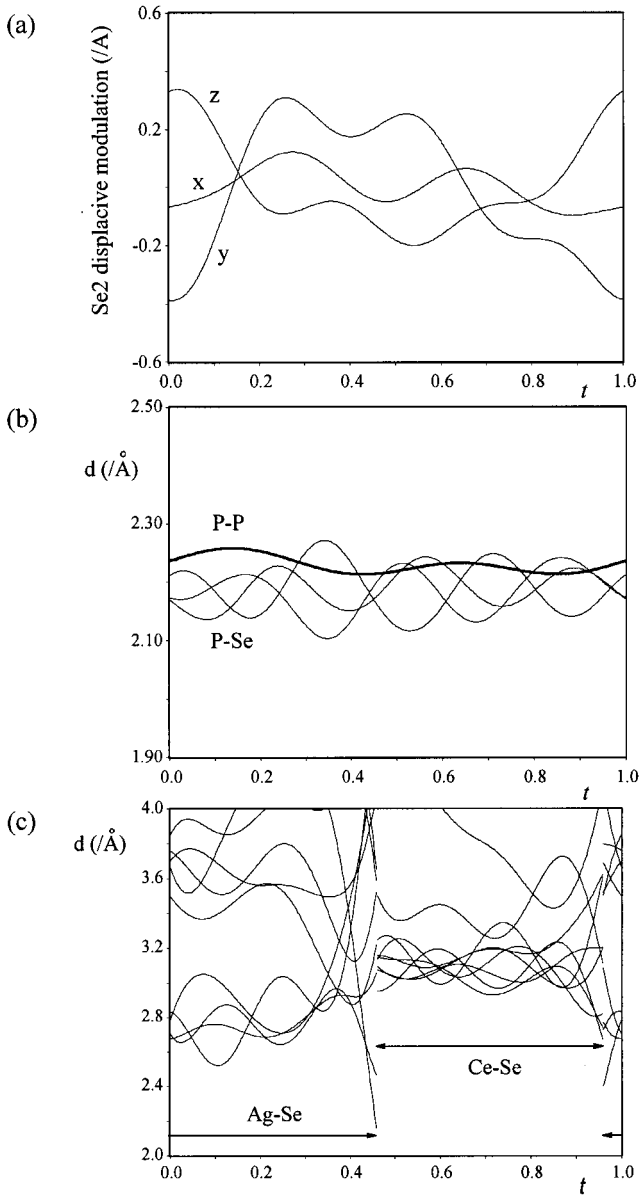

Figure 9. (a) The displacive modulation (in Å) of the coordinates (*x*, *y*, *z*) of the Se(2) atom as a function of the internal *t* coordinate, (b) modulation of the P−P (thick line) and P−Se (thin line) distances (in Å), and (c) modulation of the Ag−Se and Ce−Se distances (in Å) as a function of the internal *t* coordinate for the incommensurately modulated structure of $AgCeP_2Se_6$.

versus energy using the data points at the absorption edge region of $Ce_{1.33}P_2Se_6$ are provided in Figure 11. The (absorption)$^{(1/2)}$ versus energy plot is nearly linear for all three compounds, while the plot of (absorption)^2 versus energy deviates significantly from linearity, suggesting that all three compounds are indirect band gap semiconductors. This method of determining the nature of the band gap in semiconductors has been supported by electronic band structure calculations in the case of both $K_2CuP_3S_9$[58] and Li_2PbGeS_4.[59]

The Raman spectra were obtained on single-crystal samples of the four compounds reported here, see Figure 12 and Table 6. The most striking feature of the spectra is the very strong peak at ∼220−224 cm^{-1}. By analogy, this very strong peak can be unambiguously assigned to the A_g

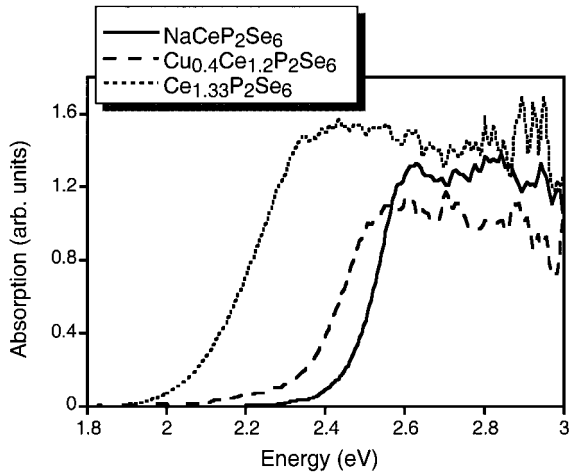

Figure 10. (a) Optical transmission spectra converted to absorption for a single crystal of $NaCeP_2Se_6$ (solid black line), $Cu_{0.4}Ce_{1.2}P_2Se_6$ (line with large dashes), and $Ce_{1.33}P_2Se_6$ (line with smaller dashes).

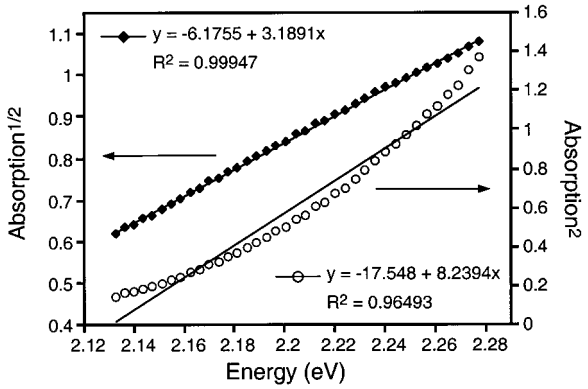

Figure 11. The absorption edge data of $Ce_{1.33}P_2Se_6$ plotted as absorption^2 versus energy (direct gap) and absorption$^{1/2}$ versus energy (indirect gap). The nearly linear dependence of the latter is consistent with an indirect band gap for $Ce_{1.33}P_2Se_6$.

stretching mode of $[P_2Se_6]^{4-}$ ligand. This dominating stretch is of diagnostic value for this anion and exists in other compounds with related structures: 215 cm^{-1} for $Pb_2P_2Se_6$,[60] 222 cm^{-1} for $Mg_2P_2Se_6$,[61] 224 cm^{-1} for $Ca_2P_2Se_6$[61], 226 cm^{-1} for $Ba_2P_2Se_6$,[61] and 225 cm^{-1} for $KPrP_2Se_6$[16c]. The remaining peaks can be tentatively assigned based on comparison with the spectrum of $Mg_2P_2Se_6$, see Table 6.

Concluding Remarks

Four new selenophosphates have been discovered, namely $NaCeP_2Se_6$, $Cu_{0.4}Ce_{1.2}P_2Se_6$, $Ce_{1.33}P_2Se_6$, and $AgCeP_2Se_6$. The synthesis of these materials was very challenging due to the high thermodynamic stability of $CeSe_2$, Cu_3PSe_4, and $Ag_4P_2Se_6$. $NaCeP_2Se_6$ possesses a layered structure which is isostructural to that of the $KLnP_2Q_6$ family of compounds, where Ln = La, Ce, and Pr for Q = Se and Ln = La for Q

(57) Pankove, J. I. *Optical Processes in Semiconductors*; Dover Publications: New York, 1971; pp 34−42.
(58) Hanko, J. A.; Sayettat, J.; Jobic, S.; Brec, R.; Kanatzidis, M. G. *Chem. Mater.* **1998**, *10*, 3040−3049.
(59) Aitken, J. A.; Larson, P.; Mahanti, S. D.; Kanatzidis, M. G. *Chem. Mater.* **2001**, *13*, 4714−4721.
(60) Becker, R.; Brockner, W.; Schäfer, H. *Z. Naturforsch.* **1984**, *39a*, 357−361.
(61) Pätzmann, U.; Brockner, W.; *Z. Naturforsch.* **1987**, *42a*, 515−516.

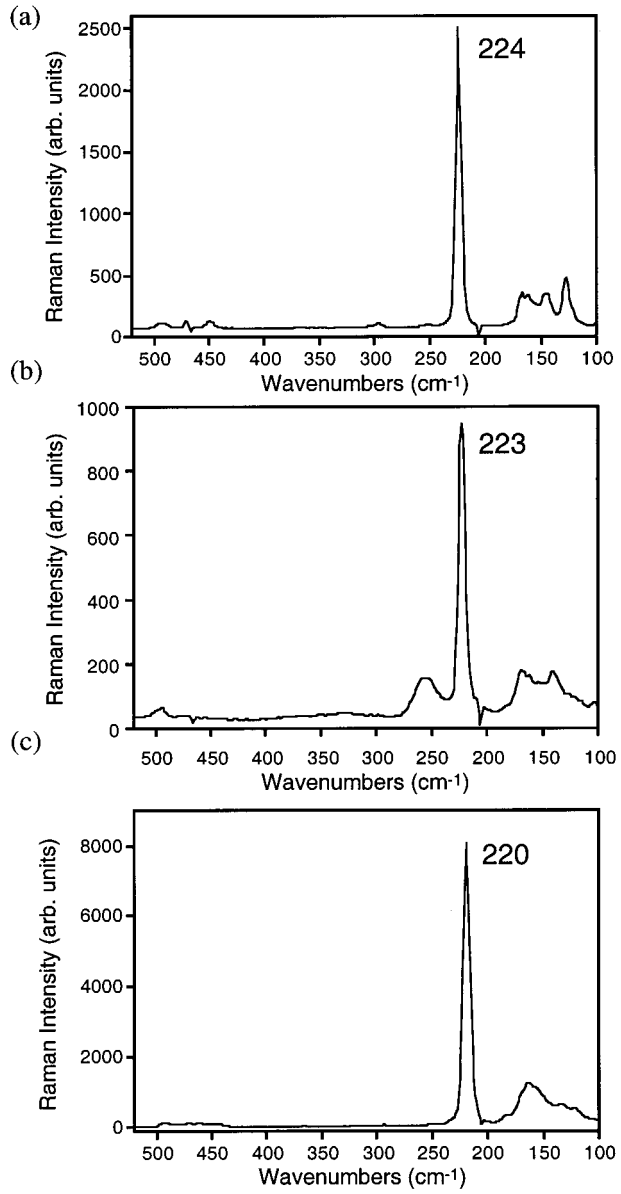

Figure 12. Raman spectra of (a) $NaCeP_2Se_6$, (b) $Ce_{1.33}P_2Se_6$, and (c) $AgCeP_2Se_6$.

= S. Substitution of the alkali metal by Cu and Ce, Ce alone, or Ag results in the formation of $Cu_{0.4}Ce_{1.2}P_2Se_6$, $Ce_{1.33}P_2Se_6$, and $AgCeP_2Se_6$. The structure of all four compounds and that of the $KLnP_2Q_6$ family can be derived from the monoclinic-II, $M^{II}PQ_3$ structure type by a substitution of the 2+ metal by a 3+ and 1+ metal or a 3+ metal and vacancies. This structure seems to be highly stable since it can accommodate cations of different size and charge, such as, main group metals, alkaline earth metals, alkali metals + lanthanide metals, late transition metals + lanthanide metals, and lanthanide metals alone. This kind of structural and compositional flexibility has already been clearly demonstrated for the $M^{II}PQ_3$ compounds of the hexagonal- and monoclinic-I-types.[62] Therefore, it seems plausible that several other phases, containing mixtures of the cations described above, could be stabilized in the structure type described here. Some of these phases could have the potential to display low-temperature phase transitions to the *Pc* structure that is known for SnP_2S_6 and $Sn_2P_2Se_6$.

Table 6. Raman Data (cm^{-1}) for $NaCeP_2Se_6$, $Cu_{0.4}Ce_{1.2}P_2Se_6$, $AgCeP_2Se_6$, and $Ce_{1.33}P_2Se_6$ Compared to that of $Mg_2P_2Se_6$, which has been Assigned Based on D_{3d} Symmetry of the $[P_2Se_6]^{4-}$ Ligand[a]

(D_{3d})	$Mg_2P_2Se_6$[61]	$NaCeP_2Se_6$	$Cu_{0.4}Ce_{1.2}P_2Se_6$	$Ce_{1.33}P_2Se_6$	$AgCeP_2Se_6$
$\nu_3(A_{1g})$	126 m−s	128 m	127 m		123 m
				142 m	135 m
				149 m	
$\nu_9(E_g)$	149 s	146 m	149 m	154 m	
$\nu_8(E_g)$	165 s	162 m	157 m	162 m	156 m
		166 m	167 m	169 m	164 m
					184 w
$\nu_2(A_{1g})$	222 vs	224 vs	224 vs	223 vs	220 vs
		252 vw	254 vw	256 m	251 vw
		296 vw	295 vw		294 vw
				330 vw,b	
					366 vw
$\nu_7(E_g)$	462 vw	450 vw	448 vw		442 vw
					463 vw
		471 vw	472 vw	470 vw	471 vw
$\nu_1(A_{1g})$	511 w	494 vw	494 vw	495 vw	495 vw

[a] Where vs = very strong, m = medium, w = weak, vw = very weak, and b = broad.

Acknowledgment. Financial support from the National Science Foundation (Grant DMR-9817287) is gratefully acknowledged. This work made use of the SEM facilities of the Center for Advanced Microscopy at Michigan State University. The Bruker SMART platform CCD diffractometer at Michigan State University was purchased with funds from the National Science Foundation (CHE-9634638). We acknowledge the use of the W. M. Keck Microfabrication Facility at Michigan State University, a NSF MRSEC facility. We would like to thank Sevane Coste from the I. M. N. for collecting the single-crystal data for $AgCeP_2Se_6$.

Supporting Information Available: An X-ray crystallographic file, in CIF format, containing information for $NaCeP_2Se_6$, $Cu_{0.4}Ce_{1.2}P_2Se_6$, $Ce_{1.33}P_2Se_6$, and $AgCeP_2Se_6$. This material is available free of charge via the Internet at http://pubs.acs.org.

IC010618P

(62) Brec, R. *Solid State Ionics* **1986**, *22*, 3−30.